ISSN 0965-545X, Polymer Science, Ser. A, 2007, Vol. 49, No. 12, pp. 1265–1283. © Pleiades Publishing, Ltd., 2007.
Original Russian Text © A.L. Volynskii, A.I. Kulebyakina, D.A. Panchuk, S.V. Moiseeva, A.V. Bol'shakova, T.E. Grokhovskaya, L.M. Yaryshevaa, A.S. Kechek'yan, S.L. Bazhenov, N.F. Bakeev, 2007, published in Vysokomolekulyarnye Soedineniya, Ser. A, 2007, Vol. 49, No. 12, pp. 2063–2084.

Structural Approach to the Study of Deformation Mechanism of Amorphous Polymers[1]

A. L. Volynskii[a], A. I. Kulebyakina[a], D. A. Panchuk[a], S. V. Moiseeva[c], A. V. Bol'shakova[a], T. E. Grokhovskaya[a], L. M. Yarysheva[a], A. S. Kechek'yan[b], S. L. Bazhenov[b], and N. F. Bakeev[b]

[a] *Faculty of Chemistry, Moscow State University, Leninskie gory, Moscow, 119992 Russia*
[b] *Enikolopov Institute of Synthetic Polymer Materials, Russian Academy of Sciences, ul. Profsoyuznaya. 70, Moscow, 117393 Russia*
[c] *Moscow State Pedagogical University, Nesvizhskii per. 3, Moscow, 119882 Russia*
e-mail: volynskii@mail.ru

Abstract—A new microscopic procedure for the visualization of structural rearrangements in amorphous polymers during their deformation to high strains is described. This approach involves the deposition of thin (several nanometers) metallic coatings onto the surface of the deformed polymer. Subsequent deformation entails the formation of a relief in the deposited coating that can be studied by direct microscopic methods. The above phenomenon of relief formation provides information concerning the deformation mechanism of the polymer support. Experimental data obtained with the use of this procedure are reported, and this evidence allows analysis of the specific features of structural rearrangements during deformation of the amorphous polymer at temperatures above and below its glass transition temperature under the conditions of plane compression and stretching, uniaxial tensile drawing and shrinkage, rolling, and environmental crazing. This direct structural approach originally justified in the works by Academician V.A. Kargin appears to be highly efficient for the study of amorphous polymer systems.

DOI: 10.1134/S0965545X07120048

INTRODUCTION

In 2007, the scientific community and, above all, the Russian polymer community is celebrating the 100th anniversary of the outstanding Soviet scientist Academician V.A. Kargin, who was the founder and father of polymer science in the Soviet Union and Russia. The life and oeuvre of this great scientist and citizen have been described in many publications [1, 2]. The authors of this brief review and the followers and adepts of Kargin will focus their attention only on one aspect of his scientific work.

This aspect concerns the structural approach proposed by Kargin to the solution of various problems of polymer science. At the end of the 1950s, Kargin had proposed several fundamental pioneering ideas concerning the structure of amorphous and semicrystalline polymers [3–5]. The proposed concepts were absolutely new and revolutionary, and their experimental verification required the use of new methods and approaches. As a basis for his approach, Kargin applied the principle of structural visualization of amorphous (structureless) polymer systems and phenomena taking place in the above systems. In his studies, he gave his evident preference to direct experimental methods, primarily, microscopic data. This approach was exceptionally fruitful and allowed obtainment of new information concerning the structure of amorphous polymers systems, including, polymer solutions [6, 7], via direct microscopic observations.

This structural approach to the study of various phenomena in polymers is the estimable heritage bequeathed by Kargin and undoubtedly deserves its further development. In this review, the authors will demonstrate the efficacy and fruitfulness of this approach to the study of structural features of deformation of amorphous polymers.

Justification of the Approach

A wide practical application of amorphous polymers should be based on a possibly deep understanding of their structural and mechanical behavior. Studies in this direction can be performed in the general way as identification and investigation of displacements of certain structural elements in polymer volume under the action of external force. According to Kargin [3–5], amorphous polymers are structurally heterogeneous systems; however, the heterogeneous character of their structure shows not phase but fluctuation and nonequilibrium character. This factor is inevitably associated with marked experimental difficulties in the study of the mechanism of structural rearrangements during deformation. The causes of these difficulties are related to the fact that, in this case, well-developed structural methods based on the phase contrast of the objects

[1] This work was supported by the Russian Foundation for Basic Research, project nos. 05-03-32538 and 06-03-32452.

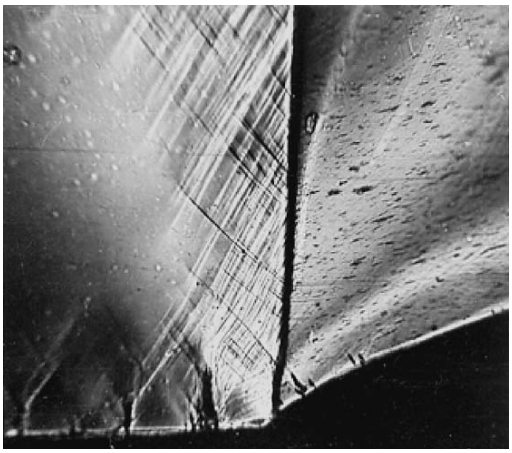

Fig. 1. Light micrograph (in crossed polarizers) of the PET sample after its deformation at room temperature via necking: neck (right-hand part) and undeformed region (left).

under study (X-ray analysis and electron diffraction analysis) appear to be inapplicable. For semicrystalline polymers, this problem has been successfully solved because structural rearrangements may be studied at the scale of crystallites [8]. Obviously, the search for new routes of visualization of structural rearrangements during deformation of amorphous polymers is a high-priority task.

Recently, a new microscopic procedure has been proposed that offers a solution to the above challenging problems and allows visualization of polymer deformation. From the experimental viewpoint, this approach is rather simple. When, prior to deformation (shrinkage), the polymer surface is decorated with a thin rigid coating, subsequent deformation (shrinkage) entails formation of a surface relief in the coating and/or its fragmentation. The character of surface structuring in the coating is controlled by the mechanism of deformation (shrinkage) of the polymer support. The proposed procedure can be successfully applied for the visualization of structural rearrangements during deformation of any solid polymers (amorphous and semicrystalline, glassy and rubbery). Below, we will demonstrate the efficacy of the proposed approach, but the principal emphasis is placed on the structural rearrangements during the deformation and shrinkage of amorphous polymers.

Visualization of Structural Rearrangements during Deformation and Shrinkage of Glassy Polymers under Uniaxial Tensile Drawing and Compression

For many years, the deformation mechanism of glassy polymers has been the subject of numerous comprehensive studies [13, 14]. Nevertheless, many aspects of deformation in glassy polymers are still unclear.

These vague aspects include the well-known abnormal structural and mechanical behavior of glassy polymers: stress relaxation and an increase in the mechanical losses in the so-called Hookean region of the stress–strain curve [13], stress growth in the deformed polymer sample under isometric heating at temperatures below glass transition temperature [15, 16], two components of thermally stimulated shrinkage of the oriented glassy polymer [17–20], accumulation of internal energy at low strains [21, 22], and unusual thermophysical properties of the deformed glassy polymers [23, 24].

To explain the above features of the structural and mechanical behavior of glassy polymers, several alternative models have been proposed [17, 18, 21, 22, 24, 25]. In our opinion, the absence of any unified standpoint concerning the deformation mechanism of glassy polymers is related to the fact that this process has been insufficiently studied by direct structural methods.

Let us characterize the inelastic deformation of a glassy polymer by using the direct microscopic data. Light microscopic examination of polymer sample during its tensile drawing allows obtainment of important information concerning the specific features of the above process. Figure 1 presents the light microscopic image of the PET sample after its deformation at room temperature via necking. As follows from Fig. 1, a part of the sample that is not transformed into an oriented state (in neck) is covered by shear bands. At first sight, the neck material does not contain any bands.

The proposed electron microscopic procedure [9–12] makes it possible to reveal important features of polymer transformation into a neck. In this case, the samples based on a glassy polymer are decorated with a thin metallic coating, and the coated samples are stretched via necking; then, the deformed samples are examined in the scanning electron microscope. As was shown in [26], fragmentation of the coating takes place in a narrow transition region between the unoriented part of the polymer sample and a growing neck. Figure 2a shows the micrograph of the polymer region localized at the interface between the neck and the unoriented part of the sample. The proposed experimental approach allows one to visualize the formed shear bands that can be easily detected with a light microscope (Fig. 1). As is well seen, the above shear bands linearly propagate throughout the transition region and are located at an angle of about 45° with respect to the direction of tensile stress.

In glassy polymers, necking proceeds via advance of the interface between the neck and the undeformed part of the polymer sample until the entire polymer material is transformed into the neck. The main fragmentation of the deposited coating is observed in the boundary region where the orientational polymer drawing takes place [26]. Figure 2b demonstrates the micrograph of the part of the deformed sample that contains the fragment of the boundary layer and the growing neck. One can easily see that shear bands formed in the boundary layer approach the neck region. The proposed

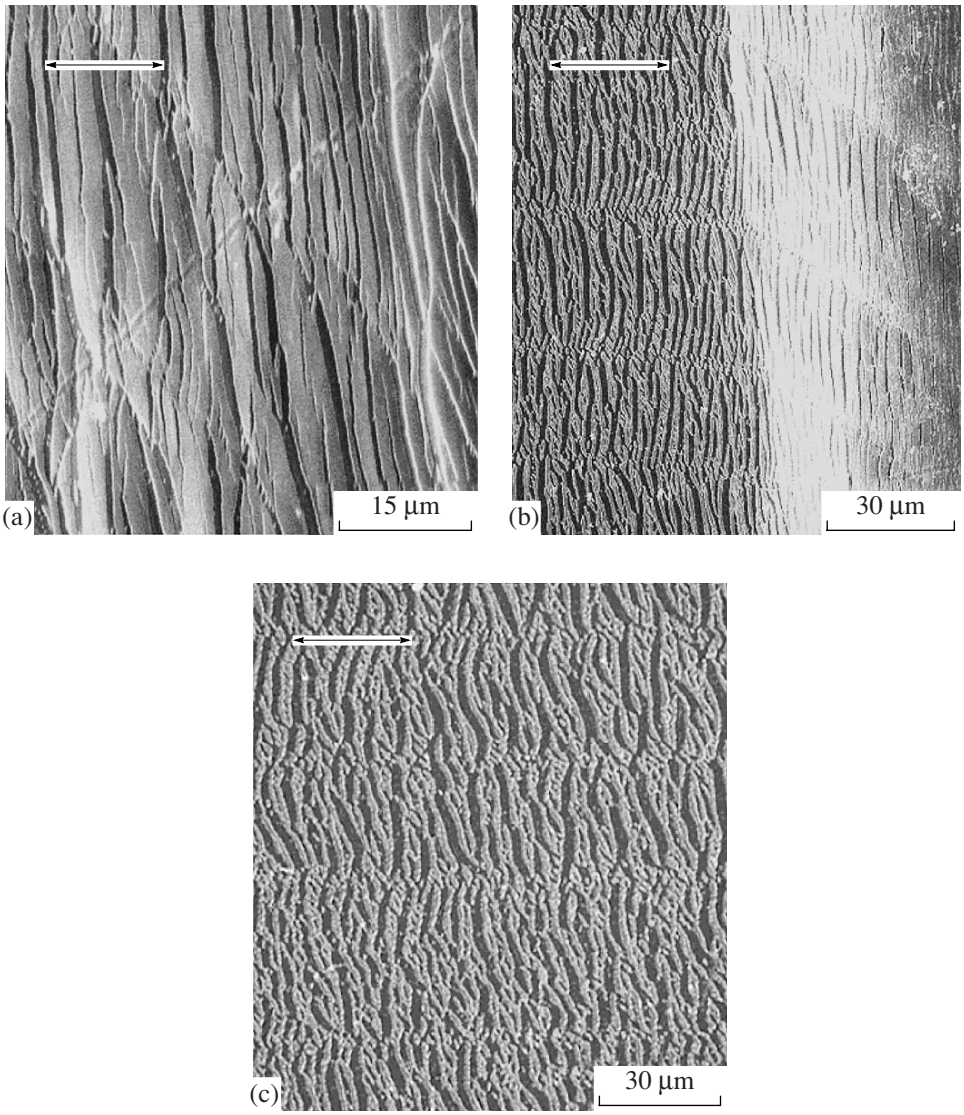

Fig. 2. SEM images of the PET sample with a thin (10 nm) platinum coating after sample stretching at room temperature via necking: (a) the region where polymer is transformed into a neck, (b) boundary region (right) and fragment of the formed neck (left), and (c) the region of the formed neck located at a certain distance from the boundary layer. Here and in Figs. 8, 10–12, and 14–16, arrows show the direction of tensile drawing.

procedure makes it possible to visualize the evolution of shear bands after their transformation (incorporation) into the neck material. In the regions where shear bands propagate into the neck, one can observe the additional fragmentation of the coating that dramatically changes its surface. When the shear bands approach the neck, they appear to lose their orientation at an angle of 45° with respect to the direction of tensile drawing. They are straightened virtually along the tensile drawing axis and are incorporated into the neck structure.

Shear bands incorporated into the neck structure are clearly seen in the regions located at any distance from the boundary zone where the polymer material is transformed into the neck (Fig. 2c). Indeed, after incorporation into the neck structure, they hardly can be termed shear bands. The point is that shear bands formed during deformation of the unoriented polymer contain the oriented fibrillar material [27]. As deformation progresses, the polymer containing shear bands is involved into the structure of the formed neck. As follows from the above results, the structure of the formed neck is heterogeneous. The neck material remembers that transition into the oriented state is performed by the polymer containing shear bands. When the neck, for example, in amorphous PET, is subjected to the shrinkage under the action of a swelling solvent, the resultant material contains a system of shear bands that can be easily detected with the light microscope [28].

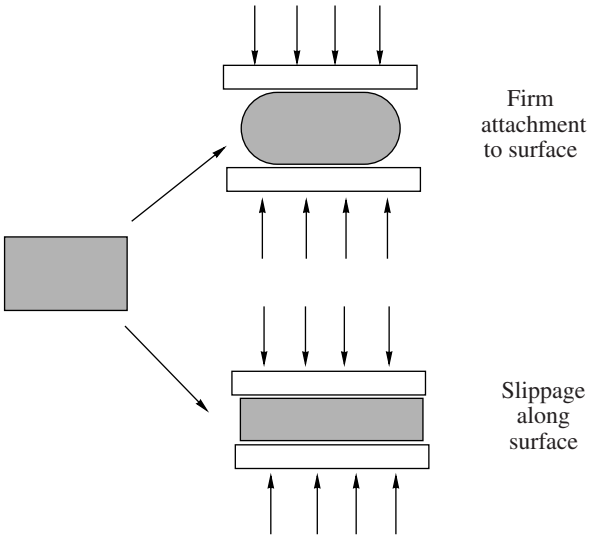

Fig. 3. Schematic representation of uniaxial compression of the polymer sample under different conditions.

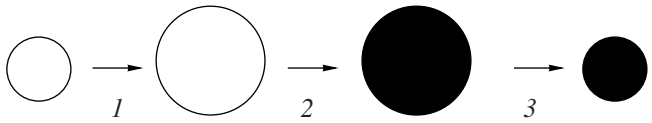

Fig. 4. Schematic representation of the experimental procedure for visualization of structural rearrangements during thermally stimulated shrinkage of the polymer sample after its deformation by uniaxial compression: (*1*) uniaxial compression, (*2*) deposited coating, and (*3*) annealing (shrinkage).

Therefore, direct microscopic observations indicate that the plastically deformed glassy polymer is characterized by a complex structure [9–12, 26]. This structure is composed of at least two components: first, the material localized in shear bands and, second, the main part of the oriented polymer, which serves as a matrix and involves the structural fragments formed in shear bands. Hence, the proposed electron microscopic procedure allows visualization of the essential structural rearrangements that accompany deformation of amorphous polymers to high strains.

To understand the general pattern of deformation, it is important to ascertain the mechanism of the reverse process—the thermally stimulated shrinkage of the deformed glassy polymer. Let us mention that, as compared with the direct deformation of polymers, information concerning these reverse processes is scarce. The point is that shrinkage of oriented polymers takes place spontaneously without any contact with measuring (controlling) units, and this process is exclusively controlled by the internal polymer properties. Let us consider the most typical results of this study obtained via the proposed microscopic procedure [9–12].

In this case, we will analyze the behavior of polymers after uniaxial compression. In many works [17–22], cylindrical polymer samples are usually subjected to the uniaxial compression under the conditions when a firm adhesion between a polymer sample and a compressing surface is provided. As a result, the cylindrical sample acquires a barrel-shaped form. In this case, the shape recovery is studied by measuring the dependence of its height on the annealing temperature. Deformation of the polymer sample for further direct microscopic studies is performed under the conditions when the sample is capable of freely sliding across the compressive surfaces. In this case, the height of the sample decreases owing to an increase in its surface area that is in contact with the compressive planes (Fig. 3). Evidently, this increase in the surface area corresponds to the transfer of some polymer material from volume to surface during deformation and, vice versa, the surface area decreases during shrinkage. This transport (mass transfer) of the polymer material during deformation is very important for understanding the mechanism of the above phenomena [29]. However, in numerous publications on this subject, this process is usually ignored and escapes any analysis.

The proposed electron microscopic procedure allows the gain of direct information concerning the mechanism of mass transfer. In particular, if shrinkage of the sample is accompanied by a decrease in its surface area, this process proceeds via polymer diffusion from surface to bulk. When the polymer sample is decorated with a thin rigid coating, this deposited coating is unable to follow the polymer surface layer on its way to the volume of the sample during shrinkage. However, owing to changes in the surface area, one can observe the relief formation that can be studied by direct microscopic observations. Evidently, the character of this relief formation reflects structural rearrangements in the deformed polymer support that are related to the mass transfer of polymer material from the surface to the bulk. Figure 4 schematically illustrates the preparation procedure of the test sample for this study.

Let us consider the process of thermally stimulated shrinkage of two PET samples: the first PET sample is deformed under uniaxial compression above the glass transition temperature (100°C), and the second sample is deformed below the glass transition temperature (at room temperature). For both samples, all other conditions were identical. Let us mention that, even though both samples are annealed at the same annealing temperature (105°C), the character of strain recovery (the temperature-induced recovery of their initial dimensions) is appreciably different. As follows from Fig. 5, the sample deformed at 100°C fully regains its initial dimensions in the temperature interval of the glass transition of PET. At the same time, the initial dimensions of the PET sample prepared by deformation at room temperature are almost completely recovered at tem-

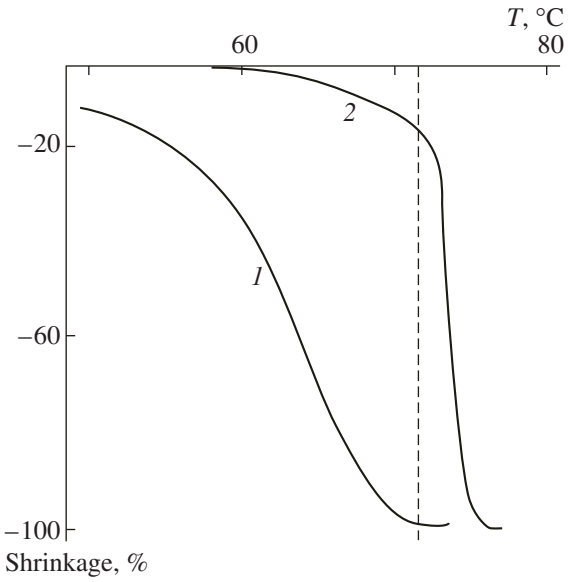

Fig. 5. Temperature-induced recovery of the initial dimensions during annealing for PET samples after their deformation under uniaxial compression at (*1*) room temperature and (*2*) 100°C.

peratures below the glass transition temperature. This thermomechanical behavior of polymer samples fully agrees with the known results [17–22].

Figure 6 shows the SEM micrographs of the deformed amorphous PET samples prepared according to the above-mentioned procedure, which illustrate the mechanism of thermally stimulated shrinkage. Figure 6 presents the SEM images for two PET samples after their temperature-induced shrinkage by the same value (22–24%). As was mentioned above, the only difference between samples a and b is the following: one sample is deformed above the glass transition temperature (100°C), and the other sample is deformed at room temperature. It is important to note that, as a result of the temperature-induced shrinkage during annealing, the surface of both deformed samples remains smooth at all stages, independently of the temperature and level of preliminary deformation.

Let us consider in more detail consequences related to the presence of the deposited coating on the surface of the polymer support during its deformation above and below the glass transition temperature. Figure 6a clearly shows that the shrinkage of the polymer sample deformed above the glass transition temperature leads to formation of a regular and well-pronounced surface relief in the metallic coating. The mechanism of formation and further development of this surface relief can be presented as a specific mode of mechanical instability (stability loss) of a rigid coating on a soft substratum under its plane compression. The mechanism of this phenomenon has been described in [30–32]. Not going into the details of the relief formation, let us mention that this relief pattern is uniform throughout the whole

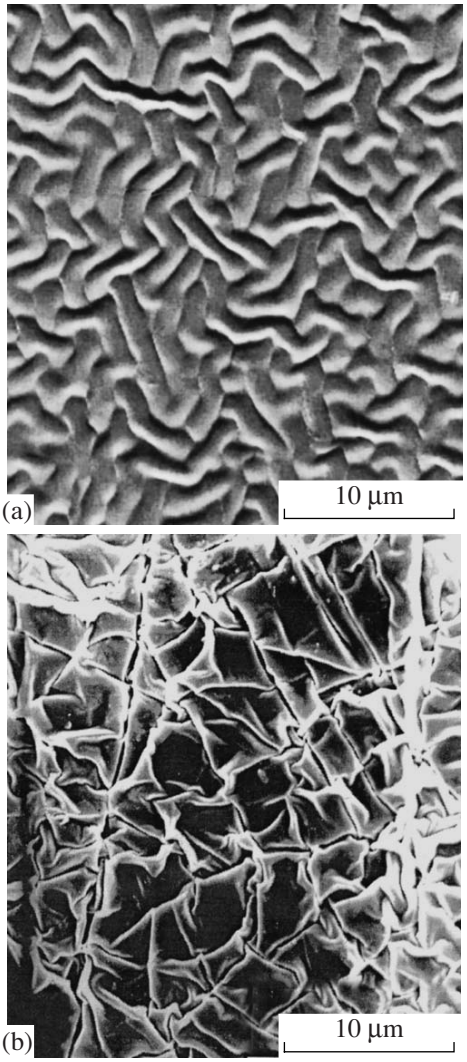

Fig. 6. SEM images of the PET samples after their deformation by uniaxial compression (a) 100°C and (b) at room temperature. After deformation, surface of the deformed samples was decorated with a thin (10 nm) platinum layer, and the coated samples were annealed at 105°C.

surface of the sample. This observation suggests that the plane deformation and, correspondingly, the shrinkage of PET samples deformed above the glass transition temperature are uniform also. In this case, the surface area of the polymer sample decreases uniformly via diffusion of the polymer material from surface to bulk. This fact indicates that the deformation of polymers above the glass transition temperature is uniform (affine). This conclusion fully agrees with the fundamental concepts of the statistical theory of high elasticity [33].

Let us consider how the deposited metallic coating affects the plane shrinkage of the PET samples deformed below the glass transition temperature [34]. As follows from Fig. 6b, the thermally stimulated strain

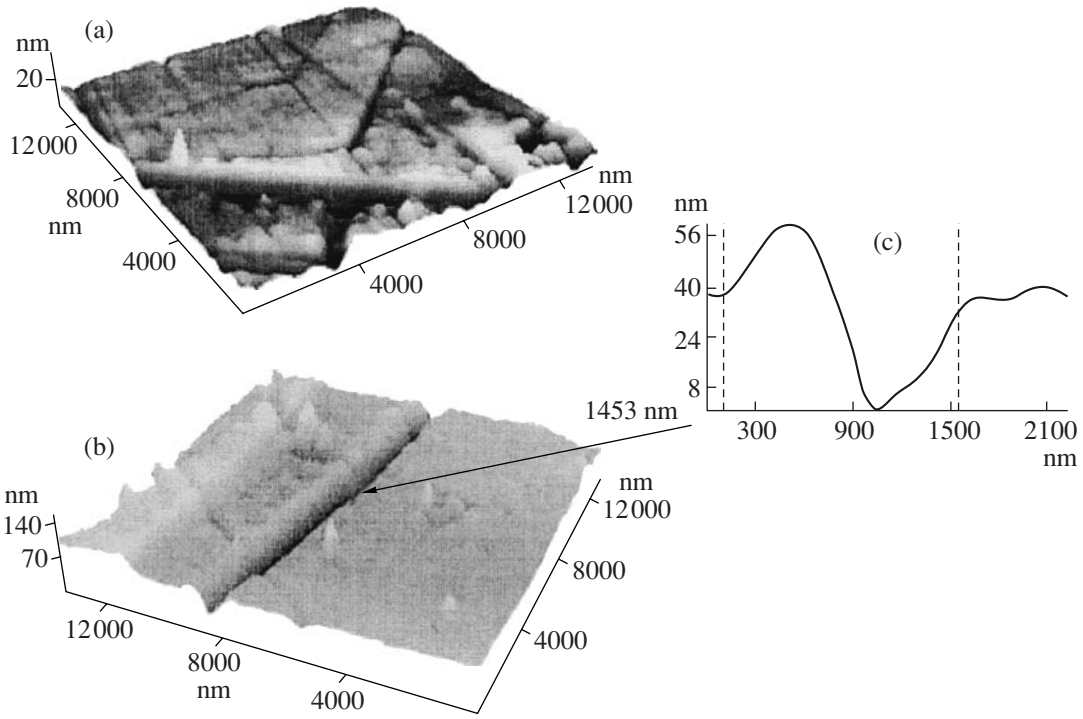

Fig. 7. Three-dimensional reconstruction of the AFM image of the surface of the PET sample after its deformation by uniaxial compression. The sample was decorated with a thin (10 nm) platinum coating and annealed; during annealing the sample underwent plane shrinkage by 18%. (a) Image size is 10×10 μm; (b) image of an individual shear band.

recovery of the sample is accompanied by appreciably different structural rearrangements in the surface layer as compared with those taking place during shrinkage of the polymer sample deformed above the glass transition temperature. At this annealing temperature, the entire surface of the polymer samples is covered with rectilinear straight bands that intersect the surface and each other at different angles. Their transverse dimensions are different, and the resultant width distribution of the above bands is broad. The AFM data (Fig. 7a) show that the above bands in the sample are grooves of various widths. With consideration for the fact that the above bands cross the whole surface of the test samples, one can assume that they intersect the cross section of the deformed sample as well. As is well seen, the wider the bands, the deeper their penetration into polymer surface, and vice versa. Within the above rectilinear grooves (Fig. 7b), the polymer is drawn from surface to bulk. In other words, in the course of shrinkage, the mass transfer of the polymer material from surface to bulk proceeds via its local diffusion in shear bands that are printed in the memory of the deformed polymer. This fact implies that, on the whole, the process of cold deformation in polymers is heterogeneous and proceeds not at the molecular level, as in the case of the deformation above the glass transition temperature, but involves the movement of large fragments of unoriented polymer, which are spatially separated by shear bands.

Therefore, the direct microscopic examination allows one to ascertain the principal structural difference between the mechanisms corresponding to the deformation of polymers above and below the glass transition temperature. The results of this comprehensive study on the deformation and shrinkage of glassy polymers by using the proposed experimental procedure make it possible to advance a new alternative mechanism for deformation of a glassy polymer that offers a consistent explanation of the above abnormal features in the mechanical, physicochemical, and thermal behavior from the unified standpoint [13–25]. In brief, this mechanism can be presented as follows. At the early stages of deformation (below and in the region of the yield point) of glassy polymers, the related deformation mechanism is controlled by the structural organization composed of two interconnected components: a part of oriented polymer localized in shear bands and the blocks of unoriented polymer. Further inelastic deformation of the polymer sample (the post-yield plateau region in the stress–strain curves) leads to the molecular orientation of polymer blocks located between shear bands. Shear bands formed at the early stages of deformation are involved into the polymer structure and preserve their individual character and characteristics until the entire polymer material is transformed into the oriented state.

When the deformed polymer sample is heated below the glass transition temperature, the polymer material

in shear bands is the first to experience shrinkage that proceeds in a wide temperature interval (the low-temperature contribution to the thermally stimulated strain recovery). Upon further heating, the main part of the oriented polymer material undergoes relaxation, and this shrinkage is virtually similar to the shrinkage of the bulk rubbery polymer and, hence, takes place in the temperature interval of glass transition (the high-temperature component of strain recovery).

Rolling

The proposed procedure for the preparation of the test samples for direct microscopic observations [9–12] allows obtainment of new information concerning the character of structural rearrangements in polymers under various deformation conditions. In particular, in [35], new data concerning the deformation mechanism of the polymer sample during its rolling below the glass transition temperature (cold rolling) were reported. Let us consider how annealing affects the behavior of the PC sample after preliminary rolling at room temperature.

Let us emphasize that, in the case of the PC sample after its rolling at room temperature, the temperature-induced strain recovery commences at the annealing temperature (~100°C). Evidently, at this temperature, the first indications of surface relief formation are observed when, prior to annealing, the surface of the polymer sample was decorated with a metallic coating. In other words, the PC sample after its rolling at room temperature is capable of certain molecular rearrangements at a temperature almost 50°C lower than its glass transition temperature.

As the annealing temperature is increased up to 110°C, far more intensive surface structuring takes place. As follows from Fig. 8a, the deposited coating makes it possible to reveal numerous shear bands that propagate on the polymer surface along linear trajectories at a certain angle to the direction of rolling. In addition to the above shear bands, the deposited coating is seen to acquire a regular wavy relief that illustrates shrinkage of the polymer sample along the direction of rolling.

When the PC samples are annealed at 120°C, a folded microrelief becomes more perfect and its folds are oriented in the direction normal to the axis of rolling (Fig. 8b). The folds of this relief become longer and more perfect, even though they are seen to be somewhat tortuous. At the same time, among regular folds of the above surface relief, one can observe the raised folds which are seen to be lighter (Fig. 8c). The detailed microscopic examination also allows identification of some new elements in the surface microrelief. As is seen, when the polymer sample is annealed at 120°C, its surface is covered by few folds that are oriented in the direction normal to the direction of primary folds or, in other words, along the direction of rolling (Fig. 8d).

When, after its cold rolling at room temperature, the PC sample with the deposited coating is annealed at 130°C, the formed surface microrelief involves two mutually perpendicular structures (Fig. 8e). This relief presents an array of regular folds that are oriented, as in the earlier case, perpendicularly to the direction of rolling. The height of some folds is higher; therefore, they overlook other folds and, in the corresponding SEM images, they appear as white bands that are oriented in the normal direction with respect to the axis of rolling. However, let us mention that the relief shown in Fig. 8e is characterized also by a well-defined system of numerous folds that are perpendicular to the direction of primary folds; in other words, they are oriented along the direction of rolling.

Finally, when the cold-rolled PC sample with the deposited coating is annealed above the glass transition temperature (155°C), the whole surface of the test sample acquires a regular microrelief with two mutually perpendicular structures (Fig. 8f). At this annealing temperature, the deformed polymer sample completely regains its initial dimensions. In addition to the structure shown in Fig. 8f, at low magnifications, one can distinguish that numerous shear bands induced in the structure of the polymer sample upon its cold rolling preserve their individual character in the surface relief that can be visualized by using the samples with the deposited metallic coating (Fig. 8g).

Hence, the proposed procedure allows visualization of a high level of structural heterogeneity of the reversible deformation in PC. Microscopic data shown in Fig. 8 make it possible to identify some unnoticed features in the structural mechanical behavior of the PC samples deformed by cold rolling at room temperature. First, virtually all inelastic deformation of the PC samples can relax below the glass transition temperature or, in other words, in the temperature interval of glassy state. This fact reflects the occurrence of certain large-scale modes of molecular motion. Relaxation of this molecular motion during annealing entails a complex evolution of internal stresses that can be easily detected by using the proposed procedure of the preparation of the test samples for microscopic studies.

Second, this relaxation can be distinctly resolved into two components. The first component of strain relaxation proceeds along the direction of rolling. The relaxation of this component commences at about 100°C. When the annealing temperature is increased to 130°C, the second component of strain relaxation comes into play. The direction of this component is normal to the direction of the first component and to the axis of rolling. As the annealing temperature is increased further, both components of strain relaxation are observed; this conclusion is confirmed by the development of two mutually perpendicular morphological forms of the microrelief in the metallic coating. This result obtained with the proposed procedure is not evident, because, during rolling, the polymer film is

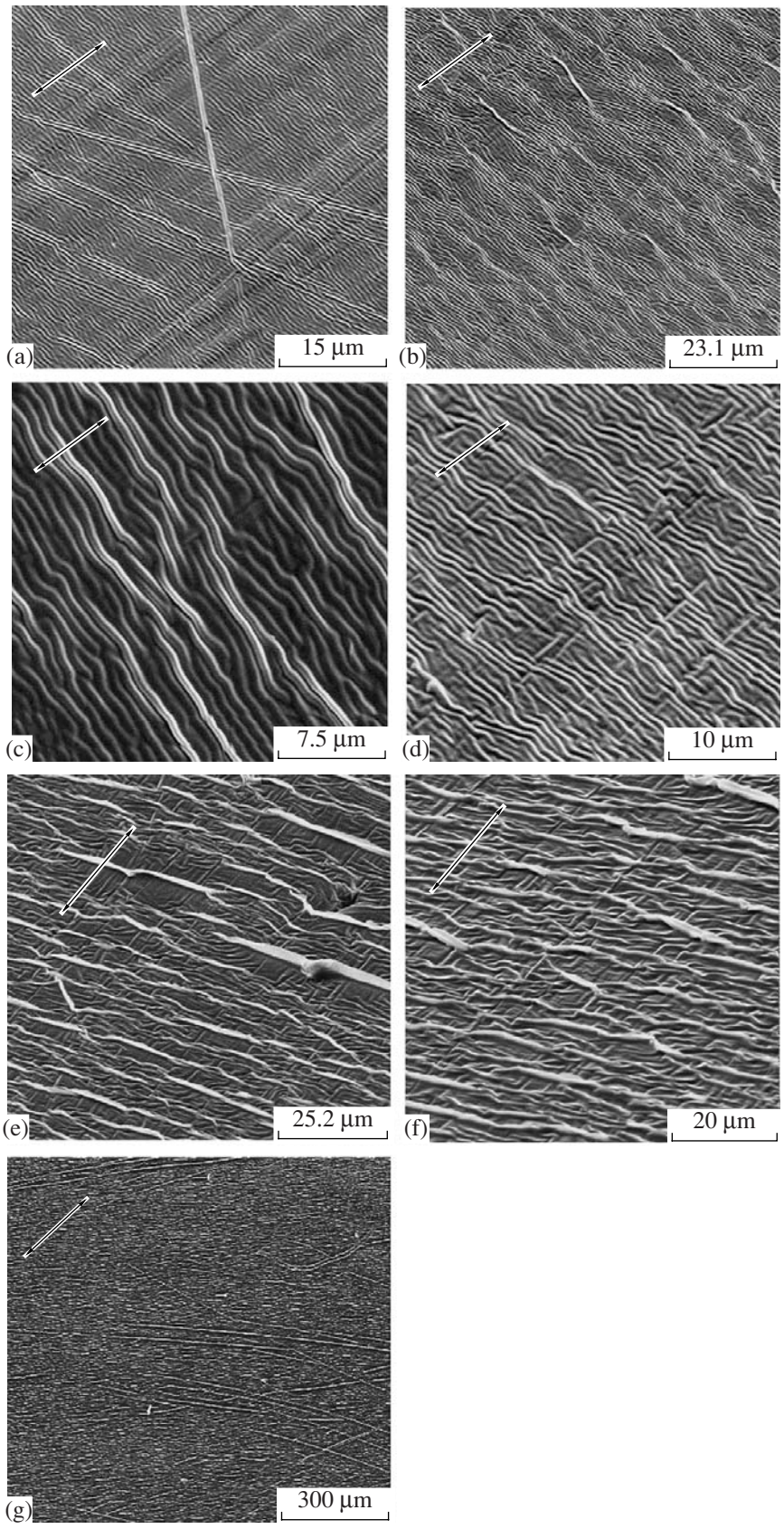

Fig. 8. SEM images of the PC samples after their deformation at room temperature via rolling, decoration with a thin (10 nm) platinum coating, and annealing at (a) 110, (b–d) 130, and (f, g) 155°C.

free in all directions along its perimeter and there are no limitations for its orientation in any direction. Nevertheless, the direct microscopic observations reveal only two deformation modes, along and perpendicular to the direction of rolling.

Solvent Crazing

The proposed procedure allowed us to gain new important information concerning the mechanism of solvent or environmental crazing. Remember that crazing is known to be a specific mode of plastic deformation in polymers. The characteristic feature of this deformation mode is the following: deformation proceeds in local regions with a well-pronounced nanoporous structure referred to as crazes [36].

Let us demonstrate advantages of the proposed procedure for studying the mechanism of solvent crazing [9–12]. Polymer samples were decorated with a thin metallic coating and stretched in the presence of adsorptionally active liquid environments (AALE); then, the solvent was removed from the volume of crazes under isometric conditions (the dimensions of the test sample were fixed). The as-prepared samples were examined on the electron microscope. Figure 9 presents the SEM images of the PET sample with a thin platinum coating after its deformation in ethanol via the mechanism of classical crazing. As follows from Fig. 9, craze growth is accompanied by an amazingly regular fragmentation in the coating and by the formation of long thin ribbons that are oriented strictly parallel to each other and perpendicularly to the direction of tensile drawing (Fig. 9b).

The regular character of fragmentation in the coating and practically the same width of the metallic ribbons seem are fascinating. In essence, regular fragments in the metallic coating can be treated as a fine measuring grid that allows estimation of the local draw ratio of polymer. In particular (Fig. 9a) one can reveal and visualize the so-called mid-rib [37], which is the region in the middle (central) part of a craze, where the local draw ratio of the polymer material is higher than that in the neighboring craze material. These regions are seen in the central part of each craze because, at the early stages of deformation, local stresses responsible for the polymer draw ratio are maximum at the craze tip. Earlier, mid-ribs in crazes have been visualized only for thin polymer films that can be studied with the transmission electron microscope.

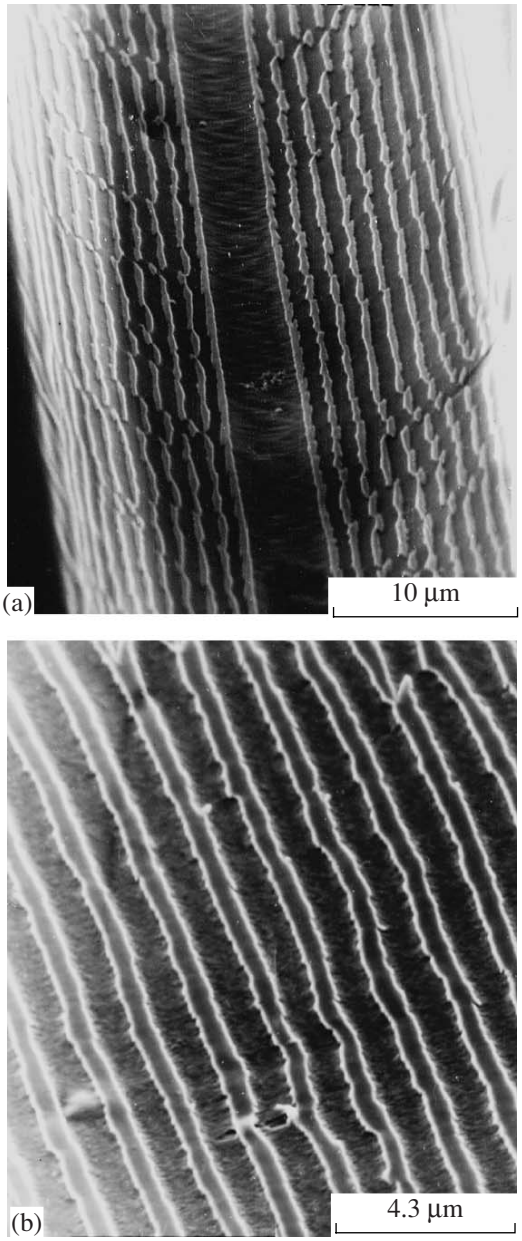

Fig. 9. SEM images of the PET samples after the deposition of a thin (10 nm) platinum coating and tensile drawing in ethanol by 50% at room temperature: (a) general appearance of a craze surface and (b) enlarged fragment illustrating fragmentation in the metallic coating.

The proposed approach makes it possible to reveal another unnoticed feature of crazing. As was found, the number of metallic fragments (ribbons on both sides of a mid-rib) is always the same. This fact implies that widening of each craze proceeds simultaneously at the same speed along both craze surfaces. This fact allows the conclusion that, in glassy polymers, craze widening is appreciably different from necking. Let us mention that the rates of neck propagation in glassy polymers (this process is quite similar to craze widening) are different in two directions. Furthermore, in the course of tensile drawing, one front of a neck advance can stop and all further process of orientational drawing is localized in one region.

Solvent or environmental crazing of polymers in the presence of liquid environments is likewise accompanied by the molecular orientation of polymers.

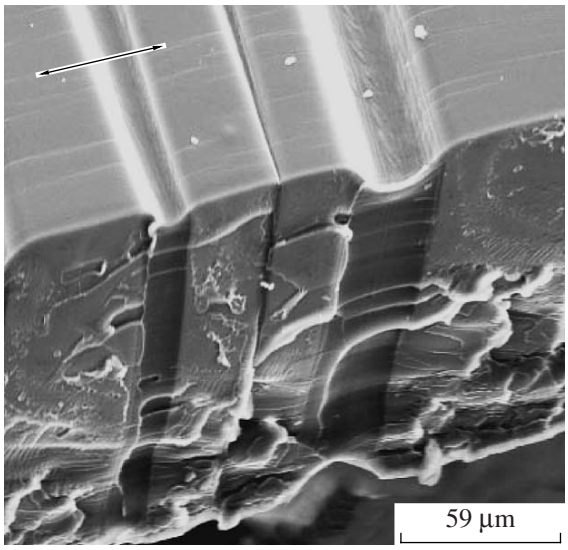

Fig. 10. SEM image of the solvent-crazed PC sample prepared by tensile drawing in AALE by 15% at room temperature.

This mode of inelastic deformation has characteristic features that are different from those of all other deformation modes. The point is that, in this case, deformation proceeds via the nucleation and evolution of microscopic regions containing the oriented fibrillar material (crazes). As a result, the deformed polymer is characterized by an inhomogeneous structure and crazes coexist with fragments of the undeformed bulk polymer [36]. Nevertheless, as in all above-mentioned cases, when the crazed samples are annealed, their initial polymer structure is fully recovered. The proposed experimental procedure makes it possible to gain new information concerning strain recovery (shrinkage) of the crazed polymer samples during annealing.

Figure 10 presents the SEM image of the solvent-crazed PC sample. In this case, crazes intersect the whole cross section of the sample. The surface of crazes and of the fragments of unoriented polymer has a well-pronounced smooth relief. To reveal (visualize) structural rearrangements taking place during annealing of the solvent-crazed PC sample, its surface was decorated with a thin (10 nm) metallic coating; then, the coated sample was annealed below (70°C) and above T_g (155°C). For microscopic studies, the samples were fractured in liquid nitrogen and examined on a scanning electron microscope.

Figure 11a shows the SEM image of the solvent-crazed PC sample after its annealing at 70°C. At this annealing temperature, one can observe a certain depression on the surface of the polymer sample, which is typical of the structure of a craze, from which AALE is removed. The low-temperature fracture surface of the test sample is smooth. Nevertheless, one can observe a fibrillar porous structure of crazes that spans inside the volume of the polymer sample. Shrinkage of the solvent-crazed samples during annealing is accompanied by structural rearrangements that can be identified by studying the surface of the craze that isolates its internal structure from the outer space (Fig. 11b). The craze surface has a folded relief that is oriented along the axis of a craze. The above folds are formed when opposite craze walls approach each other in the course of annealing. The arrangement of the folds on the craze surface is irregular, and this observation suggests that the character of shrinkage of the crazed material is inhomogeneous.

The effectiveness of the proposed procedure for the preparation of the test samples for direct microscopic observations is the most pronounced when the structure of the solvent-crazed PC samples is studied after their annealing above the glass transition temperature (155°C). As was mentioned above, at this annealing temperature, a complete healing of the crazed structure takes place. However, the deposited coating makes it possible to identify the regions where the crazes were located before annealing (Fig. 11c). Within these regions, the coating acquires a well-pronounced folded relief. At the same time, at the fractured surface, one can observe a smooth relief without any traces of crazes. This observation does not imply that, within the volume of the polymer sample, crazes experience no healing that is observed on the surface of the sample owing to the deposited coating.

However, if the test samples for microscopic observations are prepared according to the modified procedure, one can easily visualize processes taking place within the volume of the polymer sample. Figure 12a presents the SEM image of the solvent-crazed PC sample. Its temperature–stress prehistory is similar to that of the sample shown in Fig. 11a. The only difference between the samples is the following. The solvent-crazed PC sample was first fractured at low temperatures; then, the fractured surface was coated with a thin metallic layer and the coated sample was annealed under the same annealing conditions as the sample shown in Fig. 11a. As is seen, as a result of this treatment, the folded relief is formed not only on the surface of the sample annealed at 70°C but also across its cross section (at the fractured surface). This observation indicates that the shrinkage of the crazed materials in the PC sample takes place within the whole volume and not only at the surface layer of crazes. Furthermore, the fractured surface contains regular folds, which characterize fine features of the temperature-induced low-temperature shrinkage of the crazed material.

In the solvent-crazed PC samples after their annealing above the glass transition temperature (155°C), the regions with folded reliefs are observed not only on the surface of the sample but also in its volume (Fig. 12b). This evidence allows one to visualize the location of crazes at the surface and in the volume of the PC samples, even though, as a result of annealing, crazes are fully healed. At higher magnifications, one can clearly

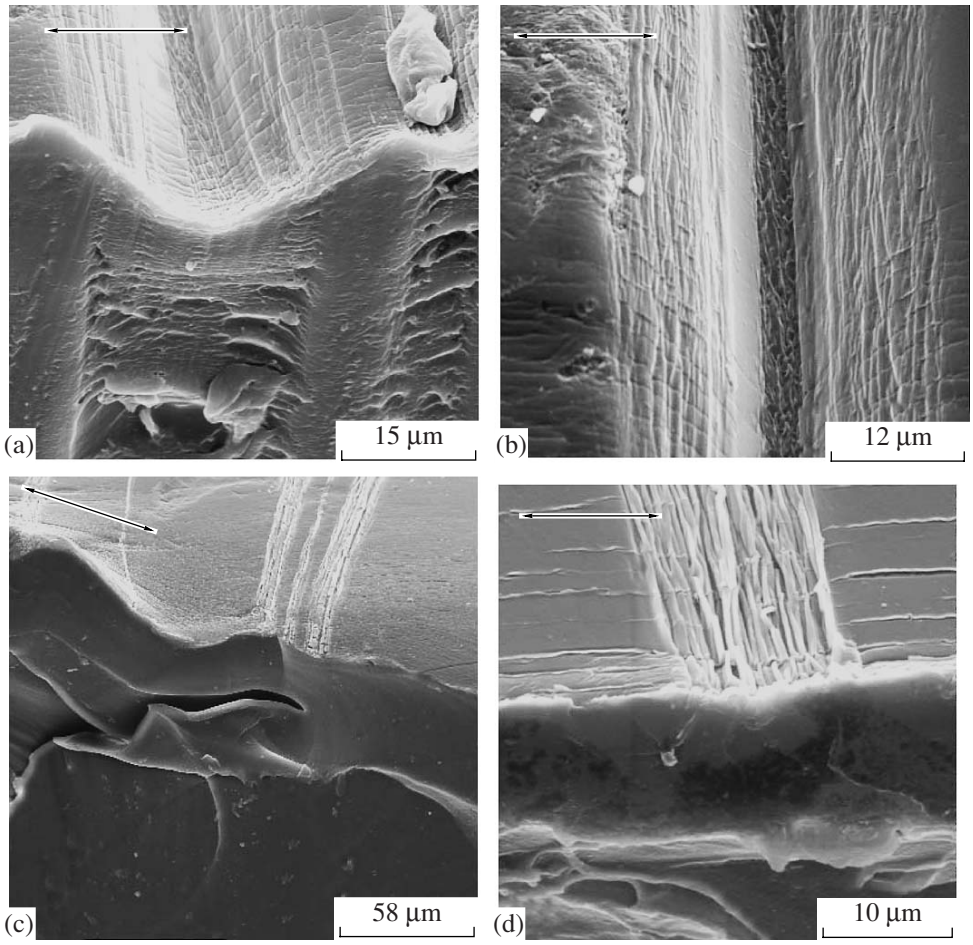

Fig. 11. SEM images of the solvent-crazed PC samples after their tensile drawing at room temperature in the presence of AALE by 17% and annealing at (a, b) 70 and (c, d) 155°C.

see that the closure of craze walls (Fig. 11d) entails a very dense packing of the folds in the coating.

The proposed experimental procedure makes it possible to reveal fine features and to study the mechanism of another phenomenon taking place during annealing of the solvent-crazed polymer samples [38]. This phenomenon is referred to as spontaneous self-elongation and can be observed for crystallizable solvent-crazed polymers. The thermomechanical behavior of this sample is quite unexpected. Figure 13 presents the corresponding thermomechanical curves of the PET samples oriented under different stretching conditions. One sample (curve *1*) was stretched in air at room temperature via necking. As expected, the annealing of this sample is accompanied by a marked shrinkage that is incomplete owing to the cold crystallization. At the same time, the solvent-crazed PET sample prepared by stretching in ethanol via the mechanism of solvent crazing is characterized by extremely unusual thermomechanical behavior (Fig. 13, curve *2*). After the stage of low-temperature shrinkage, when the annealing temperature approaches the glass transition temperature of PET, the linear dimensions of a polymer sample are increased (spontaneous self-elongation) along the direction of preliminary tensile drawing (the SSE phenomenon). It is important to mention that the SSE phenomenon takes place within a narrow temperature interval from 65–70 to 95°C. Questions concerning the mechanism of the phenomena taking place during the temperature-induced structural rearrangements in the solvent-crazed PET arise. First, what is the cause of the shrinkage of the polymer sample at temperatures below the glass transition temperature? Second, why, in the temperature region of glass transition, is this shrinkage replaced with the spontaneous self-elongation of polymer, and which factors control the temperature limits of the above phenomena? Third, what are the driving forces providing low-temperature shrinkage and self-elongation?

With due regard for the complex structure of the solvent-crazed polymer (unoriented regions alternate with crazes with fibrillar–porous structure), it is necessary to ascertain how the complex structure of solvent-crazed polymer controls changes in geometric dimensions.

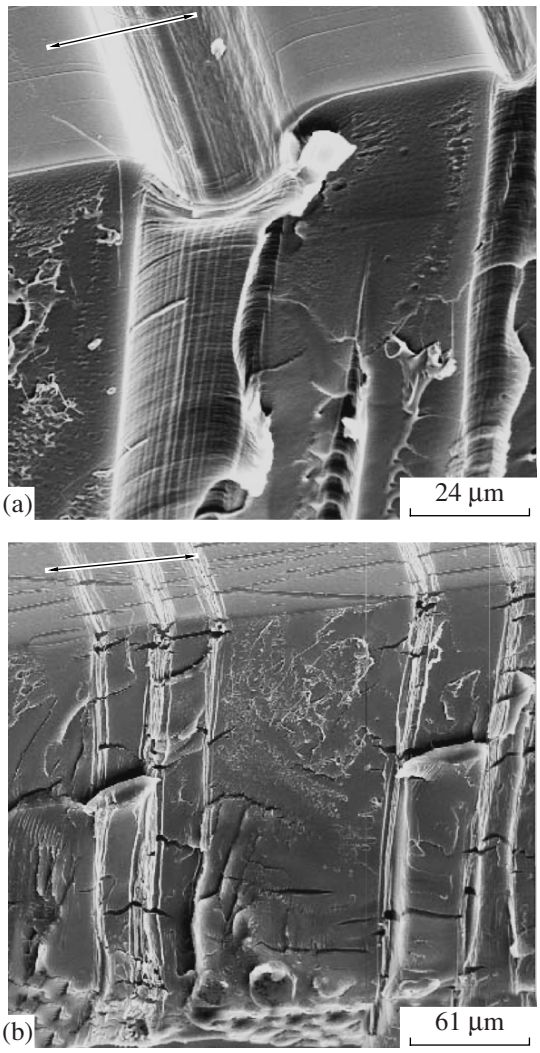

Fig. 12. SEM images of the solvent-crazed PC samples after their tensile drawing at room temperature in the presence of AALE by a tensile strain of 17% and annealing at (a) 70 and (b) 155°C. A thin metallic coating was deposited onto the test samples after their low-temperature fracture.

Figure 14 presents the electron microscopic image of the solvent-crazed PET film after its stretching by a tensile strain of 50% in the presence of adsorptionally active solvent (ethanol). The above SEM images show both surface and inner fractured structure of the sample. As is seen, the tensile drawing of PET is accompanied by the development of crazes that grow in the direction perpendicular to the direction of the applied stress and the grown crazes propagate across the whole cross section area of the sample (Fig. 14a). At the surface of each craze, craze fibrils, which are typical of craze structure, coalescence and form a monolithic top film that isolates the inner craze structure (Fig. 14b). Note that, as a result of the removal of an active liquid from the craze volume, the above thin film is saddle-shaped. Nevertheless, within the craze volume except the surface, craze fibrils formed by the oriented macromolecules, turn out to be disintegrated and form a typical fibrillar–porous structure. As follows from Fig. 14, the surface of the above thin films on the top of each craze and the surface of regions of the initial polymer between crazes have a smooth and flat relief. The above morphological features of the solvent-crazed PET samples have been found and described in detail in our earlier publications [36].

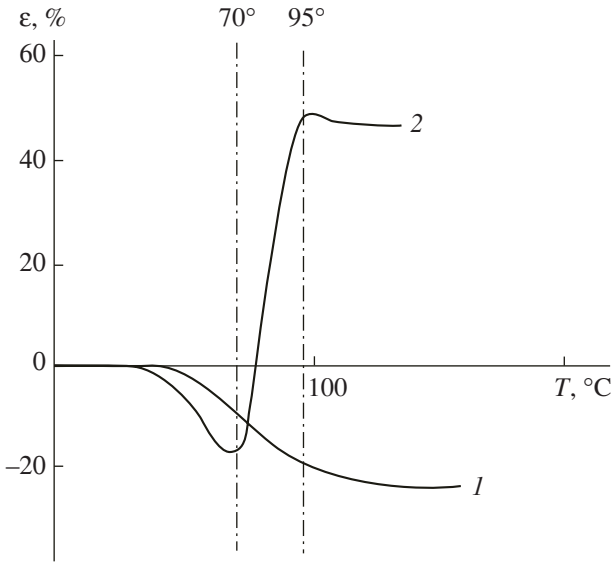

Fig. 13. Thermomechanical curves of the PET samples (*1*) after their tensile drawing in air via necking and (*2*) after stretching in ethanol by a tensile strain of 50%.

Let us now discuss which information concerning the thermomechanical behavior of polymer samples can be obtained by using the direct microscopic procedure [9–12]. In this case, the surface of the solvent-crazed PET sample (its structure is shown in Fig. 14) is decorated with a thin metallic coating and the coated sample is annealed. As was found, when the sample is annealed below the glass transition temperature or, in other words, in the temperature interval where only shrinkage of the sample is observed, the proposed procedure makes it possible to reveal the morphological rearrangements not only at the surface but also in the volume of crazes (Fig. 15). After annealing at 60°C, one can observe the formation of folds in the metallic coating only at the surface of crazes. This observation unequivocally indicates that, owing to shrinkage, craze walls come closer to each other. At the same time, the surface of polymer fragments between crazes remains smooth. This fact implies that this part of the crazed polymer sample does not contribute to changes in the dimensions of the sample and plays no role in the observed macroscopic shrinkage. This observation suggests that the low-temperature shrinkage of the polymer

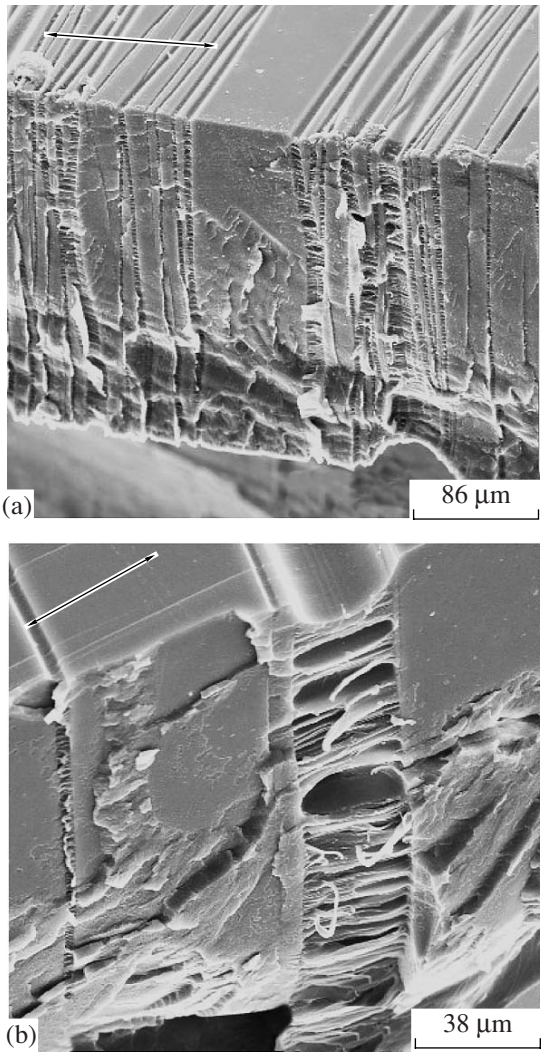

Fig. 14. SEM images of the solvent-crazed PET sample stretched in ethanol by a tensile strain of 50%. Comments are given in text.

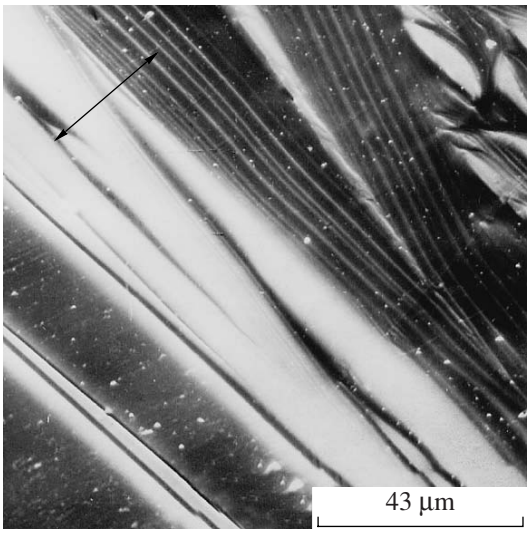

Fig. 15. SEM images of the solvent-crazed PET sample after its stretching in ethanol by a tensile strain of 50% and annealing at 60°C. Prior to annealing, surface of the sample was decorated with a thin (10 nm) platinum coating.

sample, as in the case of the solvent-crazed PC sample, is exclusively related to processes taking place within grown crazes.

When the solvent-crazed PET samples are annealed above the glass transition temperature (the temperature interval of spontaneous elongation in Fig. 13), the morphology of the sample dramatically changes (Fig. 16). First, fragments of the undeformed polymer located between crazes acquire a regular wavy relief and the folds of this relief are oriented along the direction of tensile drawing. Second, the surface of a thin film on the top of crazes appears to be covered with a regular wavy microrelief (Fig. 16b). These results indicates that these regions of the crazed polymers appear to be compressed in the direction perpendicular to the direction of tensile drawing. At high magnifications, the corresponding SEM image (Fig. 16c) clearly shows that the folds in the above regions are oriented along and perpendicularly to the direction of stretching. The regular microrelief in the regions between crazes has a fixed period that is ~2 μm. As follows from Fig. 16d, at the boundary between a craze and an unoriented polymer, this regular microrelief is transformed into another regular microrelief but with a much smaller period (~0.4 μm).

This experimental evidence allows us to propose the scenario of structural rearrangements during annealing of the solvent-crazed PET samples. The microscopic data shown in Figs. 14 and 15 indicate that shrinkage of the solvent-crazed PET below the glass transition temperature is provided by processes taking place in the volume of crazes. In this case, shrinkage is observed at temperatures well below the glass transition temperature of the bulk PET (Fig. 13). The unusual thermomechanical properties of the solvent-crazed polymers can be convincingly explained by depression in the glass transition temperature in the highly oriented material of crazes. This explanation fully agrees with the results reported in [39, 40].

Electron microscopic images shown in Fig. 16 allow the saggestion that the spontaneous self-elongation of the solvent-crazed PET samples is related to the involvement of polymer regions localized between crazes into the overall changes in geometric dimensions of the test samples. Indeed, starting at an annealing temperature of ~70°C (when the T_g of the bulk PET is attained), a regular wavy relief is formed on the surface of polymer regions located between crazes. The development of this relief indicates compression of the poly-

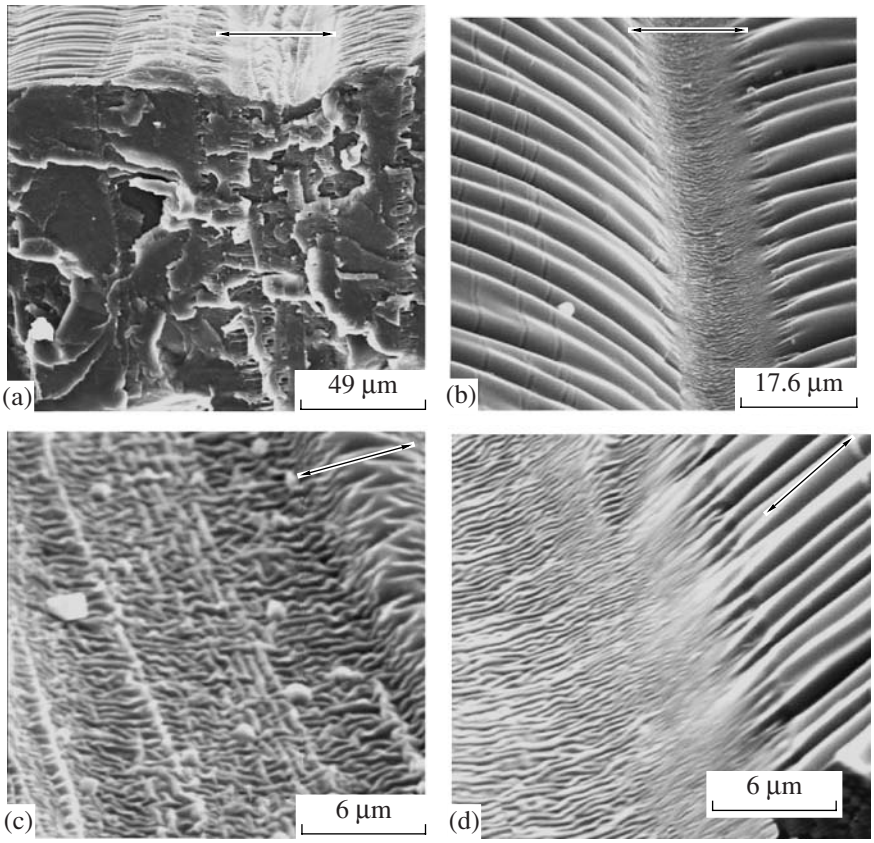

Fig. 16. SEM images of the solvent-crazed PET sample after stretching in ethanol by 50% and annealing at 170°C. Prior to annealing, surface of the sample was decorated with a thin (10 nm) platinum coating: (a) general appearance of the sample, (b, d) surface of a craze and adjacent bulk polymer material, and (c) craze surface.

mer support in the direction perpendicular to the axis of tensile drawing. At the same time, the formation of the surface relief on the above polymer regions is accompanied by the development of a similar relief on the surface of crazes (Figs. 16c, 16d). However, the period of this relief appears to be smaller by an order of magnitude. This fact suggests, in particular, that the elastic modulus of the polymer at the top of crazes is much higher than the elastic modulus of the unoriented rubbery PET between crazes. The latter conclusion is not evident and demonstrates advantages of the proposed microscopic procedure [9–12].

Therefore, shrinkage of the solvent-crazed PET samples, which commences practically at room temperature, is provided by processes taking place in crazes. This shrinkage is observed up to the glass transition temperature of PET and proceeds via closing-in movement of the walls of individual crazes. The low-temperature shrinkage of the solvent-crazed polymer is associated with the entropy contraction of a highly dispersed craze matter, whose glass transition temperature is lower than that of the bulk polymer. However, this shrinkage cannot be complete, because of the strain-induced crystallization of the oriented polymer in the bulk of crazes. As a result of this crystallization, the oriented and crystallized crazed material appears to contact the blocks of unoriented initial PET. Once the annealing temperature approaches the glass transition temperature of the bulk PET, the strain-induced crystallization commences. As a result of this crystallization, the fragments of the unoriented polymer between crazes are elongated along the direction of tensile drawing, and this process is accompanied by contraction of the sample in the normal direction.

Therefore, the above experimental evidence confirms the high effectiveness of the proposed procedure for the preparation of amorphous polymer samples for the direct microscopic visualization of deformation and its structural features. Above the glass transition temperature, deformation (shrinkage) is homogeneous and proceeds via the diffusion of polymer chains in the whole volume of the sample. Below the glass transition temperature of the amorphous polymer, deformation (shrinkage) is heterogeneous and proceeds via the displacement of rather large polymer fragments that alternate with the regions of inelastically deformed polymer (shear bands or crazes).

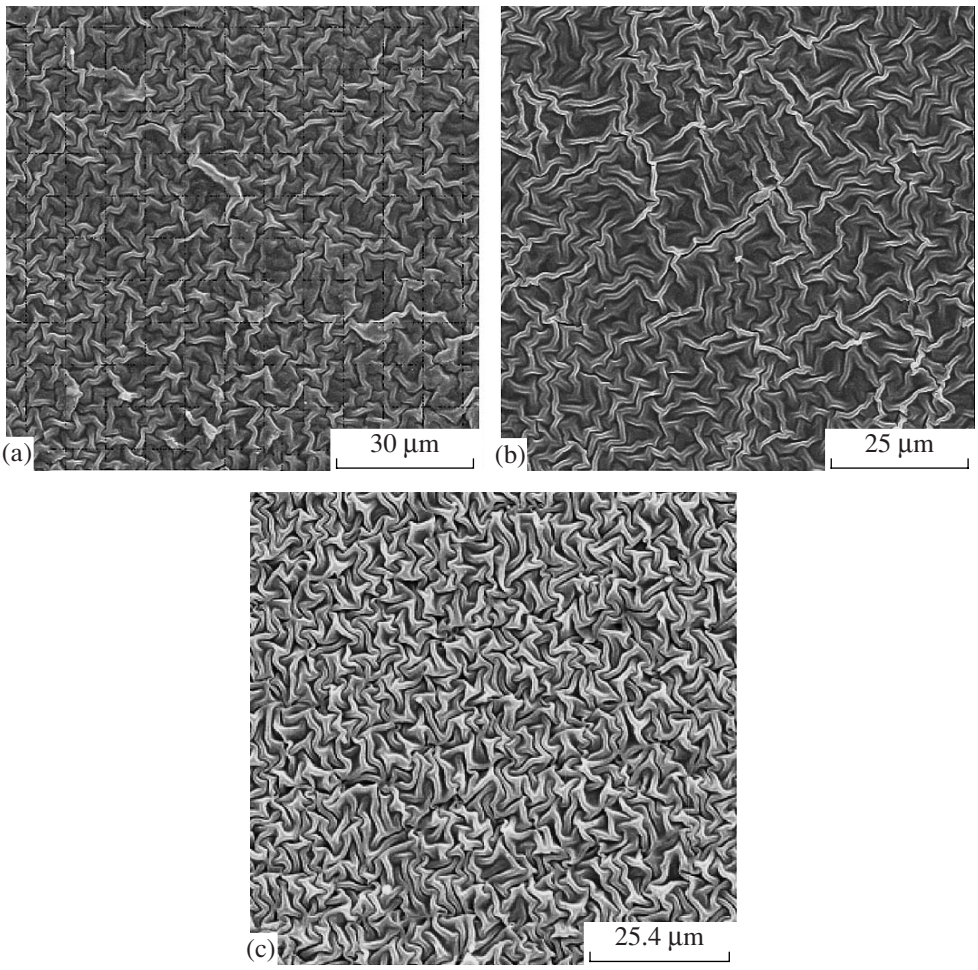

Fig. 17. SEM images of the plasticized PVC sample after its plane stretching by (a) 10, (b) 14, and (c) 27%, deposition of a thin (10 nm) platinum coating, and strain recovery.

Rubbery Deformation

The proposed visualization approach [9–12] is effective not only for gaining information concerning the deformation processes in glassy polymers. This approach is also helpful for studying the deformation processes in polymers existing in other physical and phase states (rubbery, viscous, crystalline, etc.). Obtaining adequate information on the structural rearrangements during deformation of rubbery polymers is a serious problem that is far from solution. This situation is primarily related to the fact that rubbery networks are amorphous systems, and the traditional structural methods based on the phase contrast of the test samples (X-ray analysis, electron diffraction analysis, and microscopy) are ineffective. At the same time, the proposed visualization approach [9–12] allows a gain of direct information on the type and distribution of mechanical stresses in the deformed polymer. For polymers in the rubbery state, the direct experimental evidence is missing. The deformation of rubbery polymers is assumed to be uniform (affine) [33]. Let us mention that, at the present time, no methods providing direct information concerning the stress distribution in rubbery polymers responsible for their deformation and/or shrinkage are available.

Even in pioneering work [41], the use of the proposed approach [9–12] allowed us to conclude that, in real rubbery polymers, the affine character of deformation is an exception rather than a rule. In this study, we examined the structural rearrangements during the uniaxial stretching and shrinkage of two rubbery polymers, namely, a crosslinked isoprene rubber (IR) and a plasticized PVC with a glass transition temperature of –15°C. As was found, the deformation of the above polymers is accompanied by appreciably different structural rearrangements, which can be revealed by studying the relief formation in the deposited coating by direct electron microscopic observations. The tensile drawing and shrinkage of the plasticized PVC samples decorated with a metallic coating entail the development of morphologically similar structures in the polymer surface layer. This fact confirms a relatively

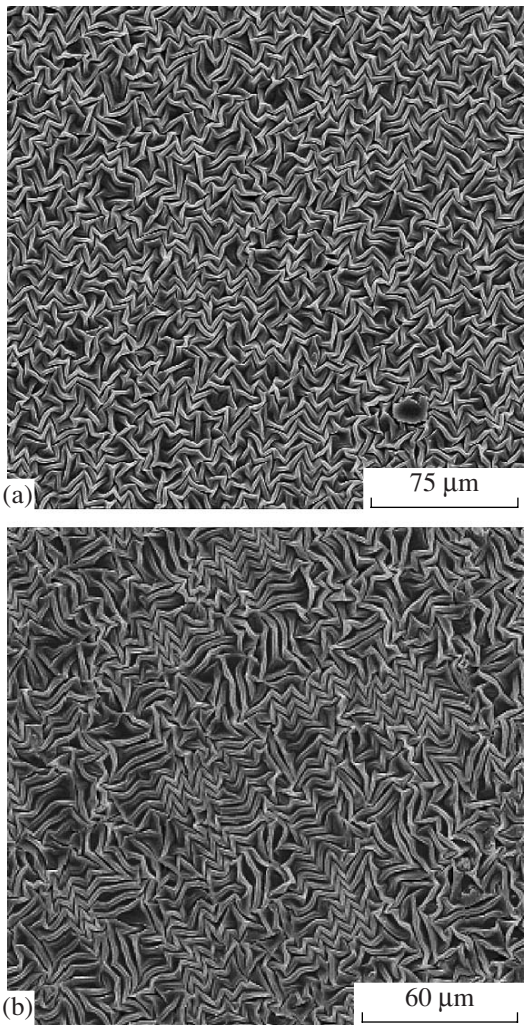

Fig. 18. SEM images of the crosslinked IR after plane stretching by (a) 5 and (b) 20%, deposition of a thin (10 nm) platinum coating, and strain recovery.

equilibrium (reversible) character of deformation. In the case of IR, direct (stretching) and reversible (shrinkage) deformation runs are characterized by different surface patterns. This difference between direct and reverse processes indicates an irreversible character of deformation and is related to different molecular mobilities of crosslinked (IR) and noncrosslinked (PVC) polymers.

In this study, we would like to demonstrate the advantages of the proposed visualization approach for the study of plane shrinkage of three rubbery polymers (plasticized PVC and crosslinked IR and NR) [42]. The above polymers were subjected to plane tensile drawing; then, the dimensions of the test samples were fixed; and the samples' surfaces were decorated with a thin metallic coating. The coated samples were released from stretching clamps thus allowing the recovery of the samples' initial dimensions.

Figure 17 presents the typical results of this study. As is seen, owing to the plane shrinkage of the stretched PVC film, the deposited metallic coating loses its stability and acquires a regular microrelief. The character of relief formation fully agrees with the morphology of the surface relief formed in the other systems under similar conditions [9, 10, 30–32]. As follows from Fig. 17a, this microrelief is composed of densely packed and irregular folds that uniformly cover the whole surface of the polymer sample. The width of the above folds is uniform and can be directly measured. As the degree of plane compression is increased, no marked changes in the morphology of the formed microrelief are observed (Figs. 17b, 17c). In this case, only the period of folds is changed because this process is accompanied by the contraction of the formed relief by analogy with the compression of accordion bellows. Therefore, the plane shrinkage of the plasticized PVC entails a decrease in the surface area of the polymer sample; hence, according to well-known laws [43, 44], the deposited coating loses its stability and acquires a regular microrelief. It is important to mention that the relief covering the whole surface of the polymer sample with the deposited coating is morphologically uniform. This result suggests a relative homogeneity (affinity) of the stress field responsible for the shrinkage of the deformed polymer and, hence, a relative homogeneity of the polymer structure.

Let us now consider the results of the study of classical elastomers—crosslinked rubbers (NR and IR) prepared according to the proposed procedure. Figure 18 presents the SEM images of the NR samples coated with a metallic layer. As is well seen, at a relatively low level of plane compression, shrinkage entails formation of a regular microrelief on the surface of the sample that is similar to that observed in PVC (cf. Figs. 17a–17c, 18a). However, at a higher level of compression (Fig. 18b), the formed microrelief shows new morphological forms. In addition to the regions with the irregular arrangement of folds, the regions with regular patterns can be distinguished. The width of these regions is 20–40 μm, they are separated by the regions with the irregular arrangement of folds, and the dimensions of these regions are virtually the same. Nevertheless, a continuous matrix is represented by the regions of disordered and irregular arrangement of folds, whereas the ordered regions are discrete and are involved in the above disordered matrix.

The above structural features are even better pronounced in the study of plane compression of the IR sample. As follows from Figs. 19a and 19b, the regions with regular folds are observed even when the level of plane compression is 5%. The size of these regions is 50 μm. Within these regions, the folds are regular and arrange in a parquet-like pattern. A similar pattern is observed at a higher level of the plane compression of the rubbery support (Figs. 19c, 19d). Note that, if,

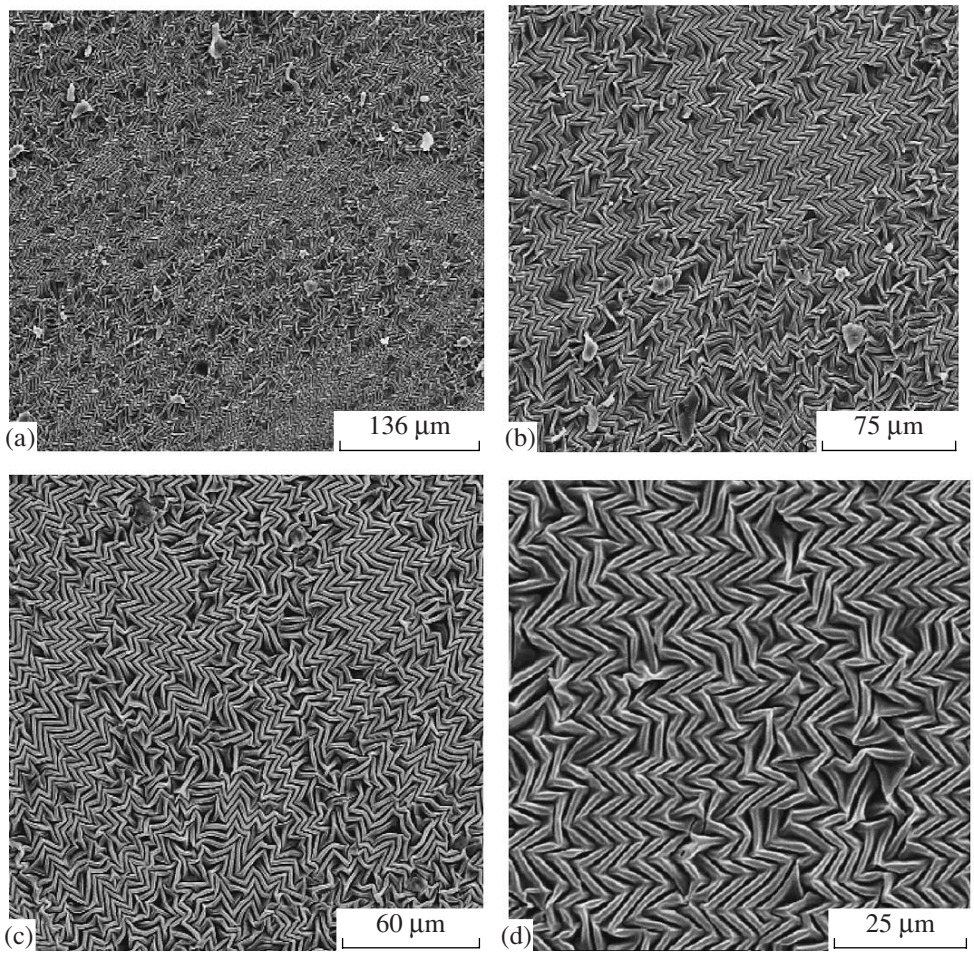

Fig. 19. SEM images of the samples based on crosslinked IR after plane stretching by (a, b) 5 and (c, d) 14%, deposition of a thin (10 nm) platinum coating, and strain recovery.

within the above regular regions, the folds are parallel to each other, the ordered regions by themselves are randomly oriented.

The above regular patterns of the surface relief formed during deformation (shrinkage) of polymer samples with the deposited thin coating actually visualize stress fields responsible for the above processes. This reasoning implies that the stress fields responsible for the shrinkage of crosslinked elastomers (IR and NR) are inhomogeneous, and this fact attests that three-dimensional structure of rubbers is heterogeneous. Furthermore, the proposed approach makes it possible to visualize and measure the dimensions of such structural inhomogeneities (20–50 μm).

As was shown in [42], this inhomogeneous character of stress fields is related to the presence of the gel fraction in the noncrosslinked IR and NR. The separation of microgels from the noncrosslinked fraction of NR by ultracentrifugation showed that their weight content is 25–30% (with respect to the net weight of NR). This evidence agrees with the results reported in [45]: during mastication of rubbers, long macromolecules experience breakdown and undergo partial crosslinking. Depending on the mastication regimes, the content of the gel fraction can achieve 60% with respect to the net weight of the initial NR. Therefore, the prebroken rubber (plasticate) contains both linear polymer and the fraction of crosslinked microgels (the gel fraction). Evidently, owing to subsequent vulcanization, the induced topological inhomogeneity is fixed. Furthermore, as a result of vulcanization, the structure of the polymer network can involve additional irregularities provided by the heterogeneous distribution of crosslinking agent [46].

Evidently, the heterogeneous character of rubbery network affects the stress–strain characteristics of the resultant materials, their ability for swelling, sorptional properties, and permeability. In this context, collection of information on the structural heterogeneity of rubber networks is crucial. The proposed microscopic procedure allows direct visualization of the deformation of rubbery polymers and tirns out to be very sensitive to

the structural (three-dimensional) heterogeneity of the deformed elastomer. This approach makes it possible not only to ascertain the structural (topological) heterogeneity of rubber networks but also to estimate the dimensions and localization of structural inhomogeneities.

Therefore, the direct structural approach advanced in the pioneering works by Kargin for the analysis of the processes taking place in amorphous polymers and related systems remains highly efficient and important. In particular, the development and use of modern methods for the direct microscopic investigation of the structure and structural evolution of the deformed polymer systems make it possible to gain new evidence and draw justified conclusions concerning the mechanism of occurring phenomena.

ACKNOWLEDGMENTS

We express our sincere gratitude to V.A. Kabanov and E.F. Oleinik for fruitful scientific discussions and valuable comments.

REFERENCES

1. V. A. Kargin, *Selected Works* (Nauka, Moscow, 1981) [in Russian].
2. *Academician Valentin Alekseevich Kargin. Recollections and Materials* (Inst. Org. Khim., Ross. Akad. Nauk, Moscow, 1996) [in Russian].
3. V. A. Kargin and G. L. Slonimskii, Usp. Khim. **24**, 785 (1955).
4. V. A. Kargin, A. I. Kitaigorodskii, and G. L. Slonimskii, Kolloid. Zh. **19**, 131 (1957).
5. V. A. Kargin and G. L. Slonimskii, *Short Essays on Physical Chemistry of Polymers* (Khimiya, Moscow, 1967) [in Russian].
6. V. A. Kargin, S. Kh. Fakirov, and N. F. Bakeev, Dokl. Akad. Nauk SSSR **159**, 885 (1964).
7. V. A. Kargin, N. F. Bakeev, S. Kh. Fakirov, and A. L. Volynskii, Dokl. Akad. Nauk SSSR **162**, 851 (1965).
8. E. F. Oleinik, Polymer Science, Ser. C **45**, 17 (2003) [Vysokomol. Soedin., Ser. C **45**, 2137 (2003)].
9. A. L. Volynskii, T. E. Grokhovskaya, A. S. Kechek'yan, et al., Dokl. Akad. Nauk **374**, 644 (2000).
10. A. L. Volynskii, A. S. Kechek'yan, T. E. Grokhovskaya, et al., Polymer Science, Ser. A **44**, 374 (2002) [Vysokomol. Soedin., Ser. A **44**, 615 (2002)].
11. A. L. Volynskii, T. E. Grokhovskaya, A. S. Kechek'yan, and N. F. Bakeev, Polymer Science, Ser. A **45**, 265 (2003) [Vysokomol. Soedin., Ser. A **45**, 449 (2003)].
12. A. L. Volynskii, T. E. Grokhovskaya, V. V. Lyulevich, et al., Polymer Science, Ser. A **46**, 130 (2004) [Vysokomol. Soedin., Ser. A **46**, 247 (2004)].
13. Yu. S. Lazurkin, Doctoral Dissertation in Mathematics and Physics (Moscow, 1954).
14. *The Physics of Glassy Polymers*, Ed. by R. N. Haward and B. Y. Young (Chapman and Hall, London, 1997).
15. L. A. Laius and E. V. Kuvshinskii, Vysokomol. Soedin. **6**, 52 (1964).
16. V. I. Shoshina, G. V. Nikonovich, and Yu. T. Tashpulatov, *Isometric Method for Investigation of Polymer Materials* (Fan, Tashkent, 1989) [in Russian].
17. S. A. Arzhakov, Doctoral Dissertation in Chemistry (Moscow, 1975).
18. *Structural and Mechanical Behavior of Glassy Polymers*, Ed. by M. S. Arzhakov, S. A. Arzhakov, and G. E. Zaikov (Nova Science, New York, 1997).
19. Y. Nanzai, A. Miwa, and S. Zi Cui, JSME Int. J., Ser. A **42**, 479 (1999).
20. Y. Nanzai, A. Miwa, and S. Zi Cui, Polym. J. (Tokyo) **32**, 51 (2000).
21. E. F. Oleynik, in *High Performance Polymers*, Ed. by E. Baer and S. Moet (Hanser, Berlin, 1991), p. 79.
22. E. F. Oleinik, O. B. Salamatina, S. N. Rudnev, and S. V. Shenogin, Polymer Science, Ser. A **35**, (1993) [Vysokomol. Soedin., Ser. A **35**, 1819 (1993)].
23. J. B. Park and D. R. Uhlman, J. Appl. Phys. **44**, 201 (1973).
24. V. A. Bershtein and V. M. Egorov, *Differential Scanning Calorimetry in Physical Chemistry of Polymers* (Khimiya, Leningrad, 1990) [in Russian].
25. D. S. Sanditov and S. Sh. Sangadiev, Polymer Science, Ser. A **41**, 643 (1999) [Vysokomol. Soedin., Ser. A **41**, 977 (1999)].
26. A. L. Volynskii, T. E. Grokhovskaya, A. I. Kulebyakina, et al., Polymer Science, Ser. A **48**, 527 (2006) [Vysokomol. Soedin., Ser. A **48**, 823 (2006)].
27. J. C. M. Li, Polym. Eng. Sci. **24**, 750 (1984).
28. A. S. Kechek'yan, Vysokomol. Soedin., Ser. B **29**, 804 (1987).
29. A. L. Volynskii and N. F. Bakeev, *Structural Self-Organization of Amorphous Polymers* (Fizmatlit, Moscow, 2005) [in Russian].
30. A. L. Volynskii, T. E. Grokhovskaya, R. Kh. Sembaeva, et al., Dokl. Akad. Nauk **363**, 500 (1998).
31. A. L. Volynskii, T. E. Grokhovskaya, R. Kh. Sembaeva, et al., Polymer Science, Ser. A **43**, 124 (2001) [Vysokomol. Soedin., Ser. A **43**, 239 (2001).
32. A. L. Volynskii, T. E. Grokhovskaya, R. Kh. Sembaeva, et al., Polymer Science, Ser. A **43**, 625 (2001) [Vysokomol. Soedin., Ser. A **43**, 1008 (2001)].
33. L. Treloar, *The Physics of Rubber Elasticity* (Oxford Univ. Press, Oxford, 1949; Mir, Moscow, 1975).
34. A. L. Volynskii and N. F. Bakeev, Polymer Science, Ser. C **47**, 74 (2005) [Vysokomol. Soedin., Ser. C **47**, 1332 (2005)].
35. A. L. Volynskii, T. E. Grokhovskaya, A. I. Kulebyakina, et al., Polymer Science (in press).

36. A. L. Volynskii and N. F. Bakeev, *Solvent Crazing of Polymers* (Elsevier, Amsterdam, 1995).

37. E. Passaglia, J. Phys. Chem. Solids **48**, 1075 (1987).

38. A. L. Volynskii, T. E. Grokhovskaya, A. I. Kulebyakina, et al., Polymer Science, Ser. A **49**, 816 (2007) [Vysokomol. Soedin., Ser. A **49**, 1224 (2007)].

39. J. A. Forrest and K. Dalnoki-Veress, Adv. Colloid Interface Sci. **94**, 167 (2001).

40. J. A. Forrest, Eur. Phys. J., E **8**, 261 (2002).

41. A. L. Volynskii, T. E. Grokhovskaya, A. V. Bol'shakova, et al., Polymer Science, Ser. A **46**, 806 (2004) [Vysokomol. Soedin., Ser. A **46**, 1332 (2004)].

42. A. L. Volynskii, T. E. Grokhovskaya, A. V. Bol'shakova, et al., Polymer Science, Ser. A **48**, 1275 (2006) [Vysokomol. Soedin., Ser. A **48**, 2144 (2006)].

43. A. L. Volynskii, S. L. Bazhenov, and N. F. Bakeev, Ross. Khim. Zh. **42** (3), 57 (1998).

44. A. L. Volynskii, S. L. Bazhenov, O. V. Lebedeva, and N. F. Bakeev, J. Mater. Sci. **35**, 547 (2000).

45. A. Casale and R. Porter, *Polymer Stress Reaction* (Academic, New York, 1978; Khimiya, Leningrad, 1983).

46. L. Gonzales, A. Rodriges, A. Del Campo, and A. Marcos-Fernandes, Polym. Int. **53**, 1426 (2004).